Intensities in the Spectra of Actinyl Ions

Spiridoula Matsika and Russell M. Pitzer*

Department of Chemistry, The Ohio State University, 100 W. 18th Avenue, Columbus, Ohio 43210

Donald T. Reed

Chemical Technology Division, Argonne National Laboratory, Argonne, Illinois 60439

Received: July 19, 2000

The absorption spectra of NpO_2^+ species in aqueous solution are investigated theoretically and experimentally, and the spectrum of NpO_2^{2+} species is investigated theoretically. The spectrum of NpO_2^+ in perchloric acid solution was taken from 350 to 1350 nm. Peak positions and optical densities are reported with overall uncertainties of 0.3 nm and 3%, respectively. A more precise value for the extinction coefficient of the most intense line is reported (398 ± 4 M^{-1} cm^{-1} for the 980.2 nm line). The intensities and positions of the electronic transitions of these actinyl complexes are computed from relativistic quantum chemical theory involving relativistic effective core potentials, corresponding spin-orbit operators, and spin−orbit, graphical unitary group configuration interaction. Because all of the low-lying electronic states for the isolated actinyl ions have the same parity, the equatorial ligands must break the inversion symmetry. Thus, model calculations on NpO_2^+ with one, three, and five chloride ligands were carried out; the five-ligand spectrum was quite similar to experimental solution spectra, whereas the one-ligand and three-ligand spectra were not. Calculations on $NpO_2(H_2O)_5^+$ were then made in order to provide a close comparison with experimental results. Similar calculations on $NpO_2(H_2O)_5^{2+}$ were also carried out but were hampered by the difficulty in doing sufficiently extensive calculations to determine the ground electronic state with the ligands present. Comparisons were made, nevertheless, using both of the candidates for ground state. A simplified crystal-field theory is developed to show how the necessary symmetry-breaking orbital mixing, $5f\phi$ with $6d\delta$, occurs selectively with 5-fold coordination.

1. Introduction

The absorption spectra of neptunium species in aqueous media have long been recognized for their value as "fingerprint" spectra to identify the various oxidation states of dissolved neptunium.[1−7] These absorption spectra are complex and typically consist of bands corresponding to forbidden electronic transitions for the isolated cations. They tend to follow the Beer−Lambert law, however, so they are widely used to establish oxidation-state-specific concentrations.

The neptunyl(V) cation, NpO_2^+, is the most stable neptunium species under a wide range of conditions.[1] It is also the most important species in the subsurface chemistry of neptunium, because it is not widely hydrolyzed and is very mobile in the subsurface when present as a contaminant.

The absorption spectrum of NpO_2^+ is dominated by a $5f \rightarrow 5f$ transition at 980.2 nm (as is the isoelectronic PuO_2^{2+} ion at a somewhat shorter wavelength). The 980.2 nm band and a less intense band at 616.5 nm follow Beer−Lambert behavior[3] and are often used analytically to establish the concentration of NpO_2^+ in solution. These two bands are affected by complexation, so they are also frequently used to study the complexation behavior of NpO_2^+.

The intensities of these peaks have raised many questions, particularly about the underlying mechanism that makes the transitions allowed. Even though the intensities are high, they are not as high as for electric-dipole-allowed transitions. It has been found both experimentally and theoretically that the lowest excited states in actinyl ions have the same parity as the ground state. In this case all excitations at low energies should be electric-dipole forbidden by Laporte's rule, which states that transitions between states of the same parity are not allowed. For the particular case of NpO_2^+, which is an f^2 system, all of the states up to 23 000 cm^{-1} are $f \rightarrow f$ transitions.[8] All of these states have two *f* electrons, so they have gerade parity and the transitions are forbidden. Even the first charge-transfer states are gerade states, which makes transitions to them forbidden also. In uranyl, it has been measured[9] and calculated[10] that the first state with different parity than the ground state is at approximately 37 000 cm^{-1}. Thus, the transitions observed must gain intensity by some other mechanism.

If for some reason the symmetry changes so that a center of inversion is no longer present, the parity rule no longer applies. One way that this can happen is for the equatorial ligands to be arranged in a structure without a center of inversion. An analogous mechanism has been used for the explanation of transitions in rare-earth ions.[11,12] There is experimental evidence that this is the mechanism for the transitions in actinyl ions as well.

Ryan, in his review on the absorption spectra of actinides,[13] observed that the intensity of the transition of plutonyl near 830 nm depends on its environment. He noted without details that whenever the arrangement of ligands around actinides does not contain a center of inversion, the $f \rightarrow f$ transitions will be observed. Sevost'yanova et al.[14] and later Tananaev[15] observed that increasing the basicity of Np(V) solutions decreases the intensity of the band at 980 nm and leads to a new band at 991 nm. They attributed the new band to the formation of the

* Corresponding author. E-mail address: pitzer.3@osu.edu.

10.1021/jp002580s CCC: $19.00
Published on Web 12/06/2000

complex NpO_2OH. Sevost'yanova et al. used the optical densities of both bands to find the hydrolysis constant for NpO_2^+. Tananaev took spectra at very high pH and concluded that the lack of transitions in this region meant that the centrosymmetric $NpO(OH)_4^{3-}$ ion had been formed. Neck et al.[16] reported spectra of NpO_2^+ with different numbers of coordinated carbonate ions; the molar extinction coefficient of the band varied from 0 to 400 M^{-1} cm^{-1}. Krot and co-workers have done the most extensive work on the dependence of the intensity on the ligands.[17−23] They took spectra of crystals and solutions of NpO_2^+ and PuO_2^{2+}. Knowing the crystal structure and comparing the spectra of crystals and solutions, they discussed the coordination number of these ions in different solutions. Their most important argument is that whenever the intensity is high, a pentagonal bipyramid is the corresponding structure. Because the intensity is high in aqueous solutions, the hydration number in these ions should be five. The hydration number is an important property of actinyl ions and has received considerable study. The answers from experimental methods (X-ray absorption fine structure, XAFS)[24,25] are five or six, with no clear preference between the two.

The only attempt to assign the spectrum of f^2 dioxoactinides was done by Eisenstein and Pryce.[26] They calculated the spectrum using parameters for the spin−orbit interaction and the ligand field and fitted them to experimental data. They assumed a 6-fold crystal field. They assigned the intense peak by arguing that it is narrow due to the fact that the charge distribution does not change much going from the ground to the excited state. This can happen if the sign of the λ value (component of orbital angular momentum along the molecular axis) of only one of the electrons changes during the excitation. The corresponding transition is $^3H_{4g} \rightarrow {}^3\Pi_{2g}$. They did not give any arguments about the source of the high extinction coefficient. The same one-electron excitation occurs in the f^1 neptunyl ion. They assigned this transition, which is experimentally observed at 8168 cm^{-1}, to the $^2\Phi_{5/2u} \rightarrow {}^2\Phi_{7/2u}$ transition.[27] Using similar arguments they assigned a few more states for the f^2 and f^1 systems.

The transition energies for NpO_2^+ have been calculated earlier,[8] but in order to assign transitions with confidence the intensities are needed also. The need to assign the spectrum, in addition to the need to find the underlying mechanism for the intensities, led us to this work, where the intensities for NpO_2^+ are reported. Taking into consideration previous arguments and experimental evidence of the influence of the equatorial ligands on the intensities, we decided to include them in our calculations. Electric-dipole transition moments were calculated. Other intensity mechanisms, such as magnetic dipole, electric quadrupole, and vibronic coupling, would give low intensities[28] that should not be influenced by the equatorial ligands to such a high degree, so we did not consider them further.

Various numbers of ligands around the linear NpO_2^+ ions were tried. In section 4.1 a first attempt to remove the center of inversion was made by shortening only one of the Np−O bonds. In this case the ion has $C_{\infty v}$ symmetry instead of $D_{\infty h}$ and thus no center of inversion. Next, chloride ions were introduced in the equatorial plane. If an even number of ions is around NpO_2^+, the center of inversion remains, and electric-dipole transition moments are still zero. For this reason we calculated only complexes that have an odd number of chlorides. In sections 4.2, 4.3, and 4.4 one, three, and five chlorides were used, respectively. A complex with five chlorides is only a theoretical model to represent a 5-fold crystal field, because probably the maximum number of chlorides that can fit in the first shell around NpO_2^+ is four. In section 4.5 we report the results for NpO_2^+ with five water molecules, because much evidence supports five as the number of water molecules in the first equatorial coordination shell around NpO_2^+ in aqueous solutions.[24,29] The results obtained can be explained with a simple model presented in section 4.6. This model is also tested for the spectrum of NpO_2^{2+} surrounded by five water molecules and is found to hold.

2. Theoretical Methods

For systems containing heavy atoms ab initio calculations become difficult for two reasons; relativistic effects play an important role in heavy atoms, and a large number of electrons are present. Relativistic effective core potentials (RECPs) can address both of these difficulties simultaneously. We use RECPs from Christiansen and co-workers,[30,31] where 78 electrons for Np, 10 electrons for Cl, and 2 electrons for O have been replaced by potentials. Spin−orbit configuration interaction (SOCI) using the graphical unitary group approach (GUGA) is used to obtain the ground- and excited-state energies and wave functions.[32] The wave functions are used to obtain the transition density matrices, and thereafter the electric-dipole transition moments. The calculations are done using the COLUMBUS suite of programs[33,34] where the spin−orbit coupling was added. The basis sets are of double-ζ plus polarization quality developed using the correlation-consistent procedure.[35]

The geometry for the complexes of NpO_2^+ with chlorides or water is taken from theoretical[29] or experimental[24] results. The distance R_e(Np−(axial O)) is set to 1.81 Å, the value obtained by Hay et al.[29] from calculations on the hydrated ion. R_e (Np−Cl) is set to 2.84 Å and R_e(Np−(equatorial O)) is set to 2.50 Å, both of these values being taken from Allen et al.[24] They reported XAFS spectra for NpO_2^+ and other actinide and actinyl ions as a function of chloride concentration. At low chloride concentrations, the hydration number is five and the distance between the oxygen of water and Np is 2.50 Å, whereas for concentrations up to 10−14 M Cl^-, one chloride substitutes for one of the waters and the distance between it and the Np is 2.84 Å.

The geometry for the calculations on $NpO_2^{2+} + 5\ H_2O$ is taken from Blaudeau.[36] He used density functional theory including relativistic effects without spin−orbit coupling. The exchange-correlation generalized gradient approximation PW91 was used. The calculations were performed using the Amsterdam density functional (ADF) codes.[37−39]

In our calculations all the ligand electrons are frozen; from the NpO_2^+ and NpO_2^{2+} electrons, only the $2\pi_u$ and $3\sigma_u$ or just the $3\sigma_u$ electrons are correlated. In all chloride complexes, only the $3\sigma_u$ electrons are correlated. In the hydrated complexes and the asymmetric NpO_2^+ ion, both the $2\pi_u$ and $3\sigma_u$ electrons are correlated.

In the asymmetric NpO_2^+ ion and the NpO_2^+ chloride complexes, $f \rightarrow f$ transitions arising from the $\delta_u^1 \phi_u^1$, δ_u^2, and ϕ_u^2 configurations were calculated. For the hydrated ion the configurations $\delta_u^1 \pi_u^1$ and $\phi_u^1 \pi_u^1$ were also included. In NpO_2^{2+} the $f \rightarrow f$ transitions from the δ_u^1 and ϕ_u^1 configurations were calculated. No charge-transfer transitions were included in any calculations because these transitions are at higher energy.

There are several quantities that can be used to evaluate the intensities of absorption and emission of electromagnetic radiation by a molecule, all of which are proportional to the square of the electric-dipole transition moment. To compare theoretical and experimental intensities, the oscillator strengths

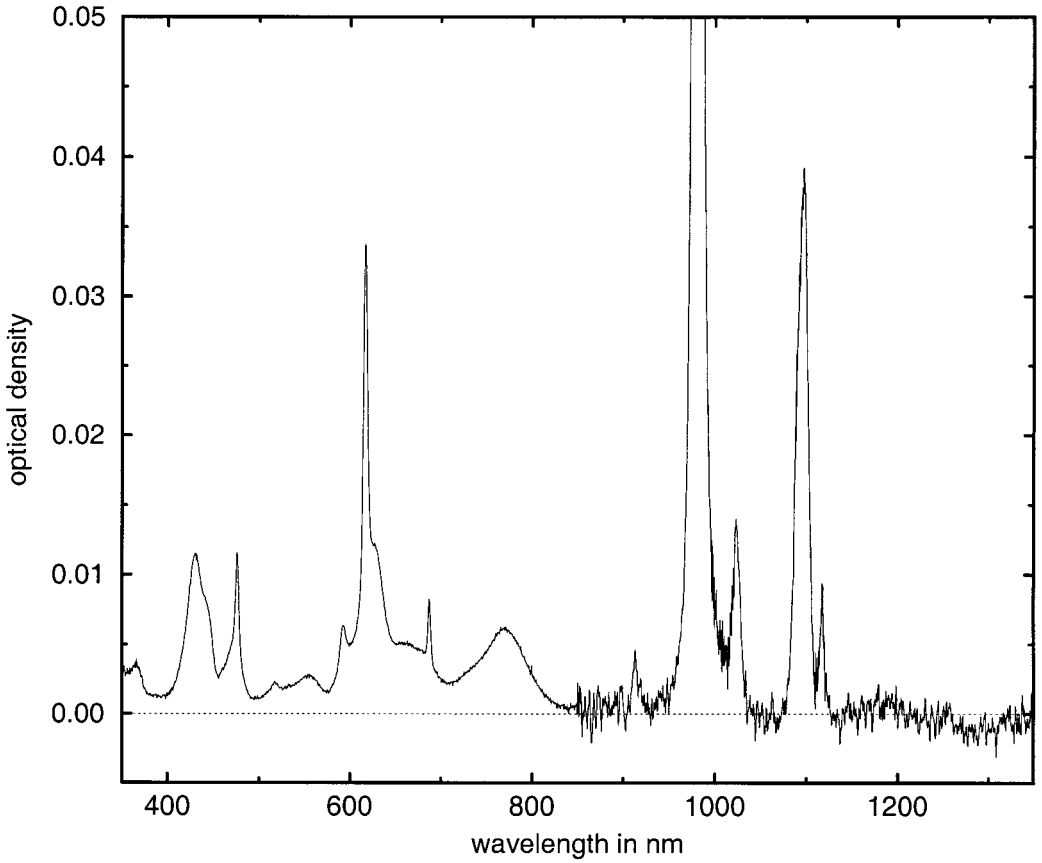

Figure 1. NpO_2^+ spectrum in 0.1 M perchloric acid solution. The optical density for the truncated peak is 0.6172.

of the transitions were calculated from the electric-dipole transition moments and the transition energies.

3. Experimental Section

3.1. Preparation of NpO_2^+. ^{237}Np, 97% purity by alpha activity, and >99% purity by mass, was oxidized to NpO_2^{2+} by fuming in perchloric acid (Aldrich reagent grade), and then reduced to NpO_2^+ by adding hydrogen peroxide and precipitating as $NaNpO_2CO_3$ by titration with 0.1 M sodium carbonate solution. The white carbonate solid was redissolved in 0.1 M perchloric acid. The pH, measured with a Ross combination electrode, was 1.69 ± 0.01 with an ionic strength of 0.1, and a concentration of 1.68 ± 0.03 mM measured by a Packard instrument 2π alpha scintillation counter.

3.2. NpO_2^+ Spectroscopy. NpO_2^+ spectra were taken at 21 ± 0.5 °C on a Varian Cary 5 spectrometer using a band-pass of 0.3 nm in the near-infrared (NIR, 850 to 1350 nm) and 1.2 nm at shorter wavelength (350 to 850 nm). Reproducibility of the spectrum was established by retaking the spectrum five times at 2-hour intervals: these spectra were indistinguishable. The accuracy of the wavelengths reported are within 0.1 nm, with an overall uncertainty of 0.3 nm in the peak positions. The optical density measurements have a maximum error of 3%. The spectrum is shown in Figure 1. No peaks were detected beyond the one at 1116.9 nm up to 1350 nm.

3.3. Extinction Coefficients. The most commonly used values for the extinction coefficients of the 980.2 and 616.5 nm NpO_2^+ bands are 395 and 22 M^{-1} cm^{-1}, respectively. These are the values tabulated in general references[1,2] but are based on the values determined by Hagan and Cleveland[3] in 2 M perchloric acid. Earlier reports[4] that these bands may not follow Beer−Lambert behavior, and hence have lower extinction coefficients, were shown to be due to the use of too large a band-pass[3,5,40] in taking the absorption spectrum. When properly resolved, and if there is no change in speciation with concentration, all of the absorption bands of NpO_2^+ follow Beer−Lambert behavior.

In obtaining the 980.2 nm extinction coefficient, the solution concentration was measured both by inductively coupled plasma mass spectroscopy and by corrected alpha activity scintillation counting. The value obtained is 398 ± 4 M^{-1} cm^{-1}, which agrees well with the most commonly cited value[3] of 395 ± 12 M^{-1} cm^{-1}. It also compares favorably to the value[41] of 387 ± 20 M^{-1} cm^{-1}.

The experimental oscillator strengths were calculated from the integrated extinction coefficients as approximated by[42]

$$\int \epsilon_\nu d_\nu \approx \gamma \epsilon_{max} \Delta\nu_{1/2} \qquad (1)$$

where ϵ_{max} is the maximum extinction coefficient, $\Delta\nu_{1/2}$ is the width at half-height, and γ is equal to 1.064 for an assumed Gaussian line shape.

4. Results and Discussion

4.1. Asymmetric NpO_2^+. One way to remove the center of inversion in NpO_2^+ is to have unequal Np−O bond lengths. Thus, calculations were carried out with $R_e(Np-O_1) = 1.73$ Å, which is the calculated bond distance for this ion,[8] for one bond length and $R_e(Np-O_2) = 1.63$ Å, a shortened bond distance, for the other bond length.

The calculated transition energies and oscillator strengths are given in Table 1. Almost all of the transitions are still forbidden, so this geometry cannot contribute significantly to the experimental spectrum.

In all of the tables of the transitions reported here, the most important $\Lambda - S$ component for every state will be given, but

TABLE 1: Transition Energies and Intensities for Asymmetric NpO_2^+

state	T_e (cm^{-1})	f (10^{-7})	mechanism
$^3H_4$	0		
$^3\Sigma^-_{0^+}$	3255	0	
$^3H_5$	4366	0	
$^3\Sigma^-_1$	4796	0	
$^3H_6$	8182	0	
$^3\Pi_1$	9116	0	
$^3\Pi_{0^-}$	9452	0	
$^3\Pi_{0^+}$	9520	0	
$^3\Pi_2$	11005	0	
$^1\Sigma^+_{0^+}$	13778	0	
$^1\Gamma_4$	14268	0	
$^1\Pi_1 + ^3\Pi_1$	16156	0	
$^3\Sigma^-_{0^+}$	20147	0	
$^3\Sigma^-_1$	22167	0	
$^1H_5$	22247	3.6	$\mu_\perp$

in some cases the mixing with other states is so heavy that less than 50% of the wave function belongs to this component.

4.2. $NpO_2^+ + Cl^-$. A single chloride ion is in the equatorial plane, at R_e(Np−Cl) = 2.84 Å (C_{2v} symmetry). Table 2 reports the calculated transition energies and intensities and whether the transition moment is parallel or perpendicular. For each state the C_{2v} double group symmetry and the most important $\Lambda - S$ component is given. There are some allowed transitions with oscillator strengths of the order of 10^{-6}. The most intense transition is to the $^1\Gamma_{4g}$ state, but its intensity is only four times higher than the next most intense transition, and this does not correspond to what is observed experimentally.

4.3. $NpO_2^+ + 3\ Cl^-$. Three chlorides were positioned in the equatorial plane in D_{3h} symmetry. The R_e (Np−O) and R_e(Np−Cl) are the same as before. In D_{3h} double group symmetry, the only states that split by the symmetry reduction from $D_{\infty h}$ double group symmetry are the ones that have $\Omega = 3, 6, 9, \ldots$ Table 3 has the states calculated up to 23 000 cm^{-1}, their double group D_{3h} symmetry, the corresponding most important $\Lambda - S$ contribution for the bare linear ion, the transition energies, and the calculated oscillator strengths for these transitions. In D_{3h} symmetry, the x, y, z components of the electric dipole moment transform as $E' + A_2''$, in order. The ground state transforms as E', so the electric-dipole transition moment to an excited-state vanishes unless the excited state transforms as A_1', A_2', E', or E''. According to these symmetry arguments, all of the transitions in Table 3 should be allowed. We can see, though, that most of the transitions have very low intensities, and their pattern does not resemble the experimental spectrum.

4.4. $NpO_2^+ + 5\ Cl^-$. Five chlorides were placed in the equatorial plane in D_{5h} geometry. In D_{5h} symmetry the states with $\Omega = 5$ split. Table 4 shows the calculated spectrum for the complex. In this symmetry the three components of the electric dipole moment transform as $E_1' + A_2''$. The ground state is an E_1' state, and the transition moment between the ground state and an excited state is nonzero only if the excited state transforms as E_1'' for parallel transitions, and A_1', A_2', or E_2' for perpendicular transitions. From the transitions in the table, the third, fourth, seventh, and tenth are forbidden by symmetry. Most of the others have some intensity. What is more interesting is that the ninth transition is more than 10 times more intense than the next most intense transition, with an oscillator strength of the order 10^{-4}. Furthermore, this transition is very close in energy to the experimentally very intense transition (10 202 cm^{-1}). Thus, our calculations suggest that although no intensity is predicted for the free ion, the one-ligand ion, and the three-ligand ion, a very intense transition appears with five ligands. This also agrees with the fact that the coordination number for this ion is believed to be close to five. Figure 2 shows plots of oscillator strengths vs wavenumbers for the complexes of NpO_2^+ with one, three, and five chlorides. The scale is the same in all plots. Only the last plot resembles the experimental spectrum.

TABLE 2: Transition Energies and Intensities for $NpO_2^+ + Cl^-$

C_{2v}	$D_{\infty h}$	T_e (cm^{-1})	f (10^{-7})	mechanism
A_1	$^3H_{4g}$	0	-	
B_2	$^3H_{4g}$	0.16	0	
A_1	$^3\Sigma^-_{0^+g}$	2999	0.2	$\mu_\perp$
A_2	$^3H_{5g}$	4516	0.5	$\mu_\parallel$
B_1	$^3H_{5g}$	4639	0	
A_2	$^3\Sigma^-_{1g}$	4648	0.3	$\mu_\parallel$
B_1	$^3\Sigma^-_{1g}$	4699	1.3	$\mu_\parallel$
B_2	$^3H_{6g}$	8617	0	
A_1	$^3H_{6g}$	8619	0.4	$\mu_\perp$
A_2	$^3\Pi_{1g}$	8929	2.8	$\mu_\parallel$
B_2	$^3\Pi_{0^-g}$	9082	4.0	$\mu_\perp$
B_1	$^3\Pi_{1g}$	9095	1.3	$\mu_\parallel$
A_1	$^3\Pi_{0^+g}$	9835	2.0	$\mu_\perp$
B_2	$^3\Pi_{2g}$	10413	13.3	$\mu_\perp$
A_1	$^3\Pi_{2g}$	10419	12.9	$\mu_\perp$
A_1	$^1\Gamma_{4g}$	13619	53.6	$\mu_\perp$
B_2	$^1\Gamma_{4g}$	13619	53.2	$\mu_\perp$
A_1	$^1\Sigma^+_{0^+g}$	14301	0	
A_2	$^1\Pi_{1g}$	16011	0.3	$\mu_\parallel$
B_1	$^1\Pi_{1g}$	16328	0.8	$\mu_\parallel$
A_1	$^3\Sigma^-_{0^+g}$	19444	6.6	$\mu_\perp$
A_2	$^3\Delta_{1g}$	21711	0.6	$\mu_\parallel$
B_1	$^3\Delta_{1g}$	21727	0	
A_2	$^3\Sigma^-_{1g}$	21865	7.0	$\mu_\parallel$
B_1	$^3\Sigma^-_{1g}$	21894	5.6	$\mu_\parallel$
A_1	$^1I_{6g}$	23559	4.6	$\mu_\perp$
B_2	$^1I_{6g}$	23559	4.4	$\mu_\perp$

TABLE 3: Transition Energies and Intensities for $NpO_2^+ + 3\ Cl^-$

D_{3h}	$D_{\infty h}$	T_e (cm^{-1})	f (10^{-7})	mechanism
E'	$^3H_{4g}$	0	-	
A_1'	$^3\Sigma^-_{0^+g}$	2566	0.6	$\mu_\perp$
E''	$^3\Sigma^-_{1g}$	4154	0.1	$\mu_\parallel$
E''	$^3H_{5g}$	4731	0	
A_2'	$^3H_{6g}$	8749	1.8	$\mu_\perp$
E''	$^3\Pi_{1g}$	8761	0.4	$\mu_\parallel$
A_1'	$^3H_{6g}$	8767	0	$\mu_\perp$
A_2'	$^3\Pi_{0^-g}$	9017	17.2	$\mu_\perp$
A_1'	$^3\Pi_{0^+g}$	9643	6.3	$\mu_\perp$
E'	$^3\Pi_{2g}$	10244	0	
E'	$^1\Gamma_{4g}$	12468	0	
A_1'	$^1\Sigma^+_{0^+g}$	13933	0	
E''	$^1\Pi_{1g}$	16185	2.2	$\mu_\parallel$
A_1'	$^3\Sigma^-_{0^+g}$	19832	99.2	$\mu_\perp$
E''	$^1H_{5g}$	22324	0.9	$\mu_\parallel$

Table 5 shows the transitions of a distorted D_{5h} symmetry. The geometry is taken from the experimentally determined structure of the $NpO_2ClO_4 \cdot 4H_2O$ crystal.[21] The five equatorial ligands in the crystal are oxygens, so in our calculations the Np−(O equatorial) distance had to be changed to the Np−Cl distance we used previously. Not all Np−Cl distances are equal but are varied the same way as in the crystal. The spectrum does not show any important changes from the D_{5h} spectrum. Some transitions that are forbidden in D_{5h} symmetry, such as the $^1\Gamma_{4g}$, start to show some intensity here. The distortion is

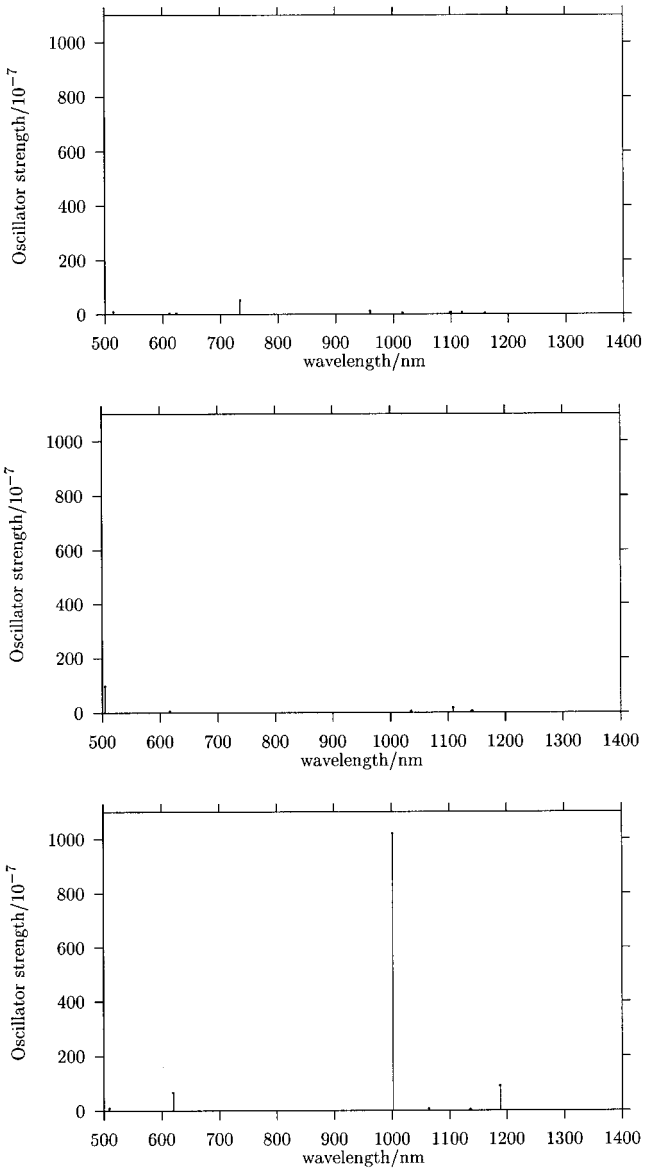

Figure 2. Calculated spectrum of NpO_2^+ with one, three, and five chlorides.

TABLE 4: Transition Energies and Intensities for $NpO_2^+ + 5Cl^-$

D_{5h}	$D_{\infty h}$	T_e (cm^{-1})	f (10^{-7})	mechanism
E_1'	$^3H_{4g}$	0	-	
A_1'	$^3\Sigma^-_{0^+g}$	2063	0	
E_1''	$^3\Sigma^-_{1g}$	3666	42.0	$\mu_{\|\|}$
A_1''	$^3H_{5g}$	4840	0	
A_2''	$^3H_{5g}$	4851	0	
E_1''	$^3\Pi_{1g}$	8418	92.1	$\mu_{\|\|}$
A_2'	$^3\Pi_{0^-g}$	8797	0.7	$\mu_\perp$
E_1'	$^3H_{6g}$	8977	0	
A_1'	$^3\Pi_{0^+g}$	9386	2.7	$\mu_\perp$
E_2'	$^3\Pi_{2g}$	9982	1021.5	$\mu_\perp$
E_1'	$^1\Gamma_{4g}$	11213	0	
A_1'	$^1\Sigma^+_{0^+g}$	13505	0	
E_1''	$^1\Pi_{1g}$	16119	67.5	$\mu_{\|\|}$
A_1'	$^3\Sigma^-_{0^+g}$	19645	12.0	$\mu_\perp$

very small, so it is likely that these transitions will have even higher intensity in more distorted environments.

4.5. $NpO_2^+ + 5\ H_2O$. To prove that the intensity pattern calculated for the 5-fold chloride crystal also holds for the hydrated ion and does not depend crucially on the ligands, we report some calculations for the hydrated ion.

TABLE 5: Transition Energies and Intensities for $NpO_2^+ + 5Cl^-$ in Distorted D_{5h} Symmetry

C_{2v}	$D_{\infty h}$	T_e (cm^{-1})	f (10^{-7})
B_2	$^3H_{4g}$	0	
A_1	$^3H_{4g}$	0.03	0
A_1	$^3\Sigma^-_{0^+g}$	2110	0
A_2	$^3\Sigma^-_{1g}$	3716	32.8
B_1	$^3\Sigma^-_{1g}$	3720	33.0
A_2	$^3H_{5g}$	4840	0
B_1	$^3H_{5g}$	4848	0
A_2	$^3\Pi_{1g}$	8458	72.6
B_1	$^3\Pi_{1g}$	8460	70.6
B_2	$^3\Pi_{0^-g}$	8833	1.0
A_1	$^3H_{6g}$	8975	0.2
B_2	$^3H_{6g}$	8993	0.6
A_1	$^3\Pi_{0^+g}$	9437	3.6
A_1	$^3\Pi_{2g}$	10044	881.6
B_2	$^3\Pi_{2g}$	10044	868.4
B_2	$^1\Gamma_{4g}$	11288	0.4
A_1	$^1\Gamma_{4g}$	11289	0.2
A_1	$^1\Sigma^+_{0^+g}$	13549	0
A_2	$^1\Pi_{1g}$	16156	48.6
B_1	$^1\Pi_{1g}$	16160	54.2
A_1	$^3\Sigma^-_{0^+g}$	19744	20.0

In these calculations five water molecules are placed in D_{5h} symmetry around NpO_2^+ as was done before with the chlorides. The molecules are perpendicular to the equatorial plane and the distance Np−(equatorial O) is set to the 2.50 Å value taken from Allen et al.[24] Hay et al.[29] found the water molecules slightly canted from the vertical positions, but that did not change the energies much (the D_5 geometry was found to be only 0.1 kcal/mol lower than the D_{5h} geometry).

The $2\pi_u$ and $3\sigma_u$ electrons were correlated. The number of double group functions was almost 10 million; this is the most correlation we could include. We found that the excited states belonging to configurations $\delta_u^1\pi_u^1$ and $\phi_u^1\pi_u^1$ appear in the energy range we are interested in, so we included them as additional references. The first calculated excited state of this type is at 13 150 cm^{-1}.

Although the transition energies are sensitive to correlation, the intensities may be less sensitive to correlation because they are calculated from the matrix elements of the electric-dipole operator, which is a one-electron operator, and of the crystal field, which is a one-electron operator to a good approximation. Many of the smaller intensities, however, depend on mixing of wave functions with high-intensity states ("intensity borrowing"), and this mixing can be sensitive to correlation.

Figure 3 shows the calculated spectrum with the energy converted to wavelength in the range from 350 to 1300 nm, in an attempt to directly compare it with the experimental spectrum. The two spectra appear qualitatively similar, but cannot be compared in complete detail because one plots oscillator strength and the other plots optical density. Apart from the intense peak at 980.2 nm (10 202 cm^{-1}) other peaks appear at 430.2, 476.1, 616.5, 686.9, 769.5, 913.1, 1022.8, 1097.0, 1116.9 nm (23 245, 21 004, 16 221, 14 558, 12 995, 10 952, 9777, 9116, 8953 cm^{-1}). Several peaks, such as the one at 616.5 nm, are complex peaks.

Experimental oscillator strengths for the peaks appearing in the spectrum in Figure 1 have been calculated and are shown in Table 7. The widths at half-height and the maximum extinction coefficients were measured and put into eq 1, setting $\gamma = 1.064$. Some widths, particularly those for complex peaks,

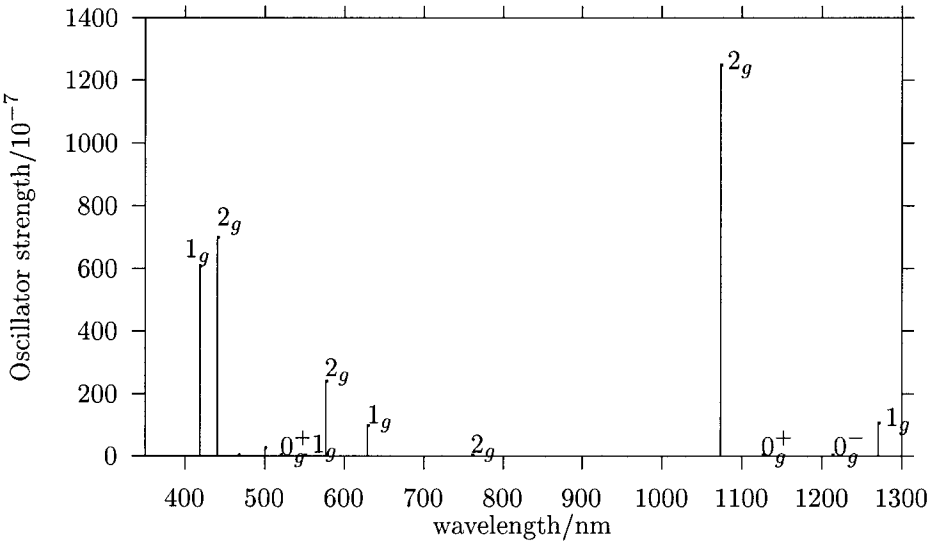

Figure 3. Calculated spectrum of $NpO_2^+ + 5\ H_2O$.

TABLE 6: Transition Energies and Intensities for $NpO_2^+ + 5\ H_2O$[a]

D_{5h}	$D_{\infty h}$	configuration	T_e (cm^{-1})	f (10^{-7})	mechanism
E_1'	$^3H_{4g}$	$\delta\phi$	0		
A_1'	$^3\Sigma^-_{0^+g}$	$\delta\delta$	1277	0	
E_1''	$^3\Sigma^-_{1g}$	$\delta\delta$	2865	48.2	$\mu_{\|\|}$
A_1''	$^3H_{5g}$	$\delta\phi$	4883	0	
A_2''	$^3H_{5g}$	$\delta\phi$	4900	0	
E_1''	$^3\Pi_{1g} + {}^3\Sigma^-_{1g}$	$\delta\phi$	7875	103.8	$\mu_{\|\|}$
A_2'	$^3\Pi_{0^-g}$	$\delta\phi$	8244	0.9	$\mu_\perp$
A_1'	$^3\Pi_{0^+g}$	$\delta\phi$	8885	0.8	$\mu_\perp$
E_1'	$^3H_{6g}$	$\delta\phi$	8993	0	
E_2'	$^3\Pi_{2g}$	$\delta\phi$	9321	1246.0	$\mu_\perp$
E_1'	$^1\Gamma_{4g}$	$\delta\delta$	9729	0	
A_1'	$^1\Sigma^+_{0^+g}$	$\delta\delta$	12704	0	
E_2'	$^3\Phi_{2g}$	$\delta\pi$	13150	0.2	$\mu_\perp$
E_2''	$^3\Gamma_{3g}$	$\phi\pi$	13743	0	
E_1''	$^1\Pi_{1g}$	$\delta\phi$	15891	94.0	$\mu_{\|\|}$
E_2''	$^3\Phi_{3g}$	$\delta\pi$	16803	0	
E_2'	$^3\Delta_{2g}$	$\phi\pi$	17346	236.2	$\mu_\perp$
E_1'	$^3\Gamma_{4g}$	$\phi\pi$	17554	0	
E_1''	$^3\Delta_{1g}$	$\phi\pi$	18177	0.8	$\mu_{\|\|}$
A_1'	$^3\Pi_{0^+g} + {}^3\Sigma^-_{0^+g}$	$\delta\pi$	19254	0.4	$\mu_\perp$
E_1''	$^3\Pi_{1g}$	$\delta\pi$	19994	23.1	$\mu_{\|\|}$
E_1'	$^3\Phi_{4g}$	$\delta\pi$	20432	0	
A_1''	$^3\Gamma_{5g}$	$\phi\pi$	20636	0	
A_2''	$^3\Gamma_{5g}$	$\phi\pi$	20655	0	
E_2''	$^3\Delta_{3g}$	$\phi\pi$	20949	0	
A_2'	$^3\Pi_{0^-g}$	$\delta\pi$	21413	0.3	$\mu_\perp$
E_2'	$^3\Pi_{2g}$	$\delta\pi$	22705	694.5	$\mu_\perp$
E_1''	$^3\Sigma^-_{1g}$	$\phi\phi$	23877	605.0	$\mu_{\|\|}$
A_1'	$^3\Sigma^-_{0^+g}$	$\phi\phi$	23886	0	
A_1''	$^1H_{5g}$	$\delta\phi$	24761	0	
A_2''	$^1H_{5g}$	$\delta\phi$	24716	0	

[a] Eight electrons were correlated.

were difficult to assign. The oscillator strength for the intense peak at 10 202 cm^{-1} is found to be 1200×10^{-7}, very close to the theoretical value of 1246×10^{-7} for the transition to the 2_g ($^3\Pi_{2g}$) state of linear NpO_2^+. The theoretical position of this peak is at 9321 cm^{-1}. There are three peaks at lower energies in both experiment and theory, with one of them being more intense than the others. This peak experimentally is located at 9116 cm^{-1} and has oscillator strength 136×10^{-7}. Theoretically the most intense peak of the three corresponds to the transition to the 1_g state ($^3\Pi_{1g} + {}^3\Sigma^-_{1g}$), is located at 7875 cm^{-1} and has

TABLE 7: Experimental Oscillator Strengths

position (cm^{-1})	ϵ_{max} (M^{-1} cm^{-1})	$\Delta\nu_{1/2}$ (cm^{-1})	f (10^{-7})
8953	6.3	36	10
9116	25	119	136
9777	9.2	96	40
10202	398	65.7	1200
10952	3.2	56	8.2
12995	3.9	755	135
14558	5.3	140	34
16221	22	181	181
21004	7.4	321	109
23245	7.5	1547	532

oscillator strength 103.8×10^{-7}. The other two appear to the left and right in the experiment but both of them are to the left in theory. The transition at lower energies corresponds to the 0_g^- ($^3\Pi_{0^-g}$) state while the one to higher energies corresponds to the 0_g^+ ($^3\Pi_{0^+g}$) state. The calculated oscillator strengths for these transitions are much smaller than the experimental ones.

The situation becomes even more complicated when looking at the transitions on the left of the spectrum (at higher energies from 10 202 cm^{-1}). We do not calculate any peak close to 10 952 cm^{-1} where there is a small experimental peak. If it is transition to an electronic state, it should be the $^1\Gamma_{4g}$ state. This is forbidden in D_{5h} symmetry, but in the distorted D_{5h} symmetry it has some intensity. In a 1-fold crystal field, as shown in Table 2, this is the most intense transition. Eisenstein and Pryce[26] attributed this feature to a vibronic excitation. The energy difference between the intense peak at 10 200 cm^{-1} and this peak is very close to the symmetric-stretch vibrational frequency (767 cm^{-1}).[43] The geometries of the two states are very similar so the Franck−Condon factor for excitation to the first vibrational level would be small, causing a significant decrease in the intensity. In the area where the broad peak appears (12 995 cm^{-1}), theoretically there is a transition to the $^3\Phi_{2g}$ state, but the oscillator strength is too small. Eisenstein and Pryce[26] argue that transitions where one of the δ_u or ϕ_u electrons is excited to a π_u orbital weaken the bond and increase the Np−O distance. We found the same effect in our calculations[8] on NpO_2^{2+}. The transition to the $^3\Phi_{2g}$ state falls into that category, so that could explain its broadening due to vibronic effects. The next two states with high calculated intensities are the $^1\Pi_{1g}$ and $^3\Delta_{2g}$. These could be the observed peaks at 14 558 cm^{-1} and 16 221 cm^{-1} respectively. The theoretical oscillator strength for the

transition to $^1\Pi_{1g}$ is higher than the experimental one for the transition at 14 564 cm^{-1}, but the theoretical oscillator strength for the transition to $^3\Delta_{2g}$ is close to the experimental one at 16 221 cm^{-1}. The peaks at 21 004 and 23 245 cm^{-1} correspond to the calculated $^3\Pi_{2g}$ and $^3\Sigma^-_{1g}$, although the intensities do not match closely. It should be mentioned here that Eisenstein and Pryce, using their simple arguments, assigned the same states as we do for the four states at lower energies. At higher energies their assignments deviate from ours.

We have calculated states up to about 24 000 cm^{-1}. The charge-transfer states start to appear near this point according to our calculated results.[8] Since we do not include these states in the calculations here, we do not make assignments at higher energies.

This is a limited investigation of the electronic spectrum of NpO_2^+ in that we only considered electric-dipole transitions in a static model (only pure electronic transitions) with perfect D_{5h} symmetry. Even within this model the calculations had very little electron correlation. Any deviation from this simple model could change the transitions. Increasing the level of the correlation treatment will affect both the line positions and the extent to which wave functions of the same double-group symmetry mix to give intensity borrowing. Nevertheless, we are able to make qualitative predictions of the most important features of the spectrum. There is little doubt that the observed very intense peak corresponds to the transition to the $^3\Pi_{2g}$ state. The following section gives a simple theoretical model that aids in understanding the pattern and mechanism of the calculated results and provides a basis for making predictions for similar systems.

4.6. Theory of Intensities. To understand the pattern of our computed intensity results, we develop a perturbation treatment of the isolated actinyl ions by the crystal field of the equatorial ligands. We do not attempt to make this simpler theory quantitative because (1) we already have more accurate results, and (2) developing an accurate one-electron crystal-field potential for nearest-neighbor ligands is a difficult problem which we have not attempted to solve.

It was pointed out by Eisenstein and Pryce[26] more than 30 years ago that excitation from the ground state of the f^2 ions, NpO_2^+ and PuO_2^{2+}, to the $^3\Pi_{2g}$ state involves excitation of a single electron. The ground state is $^3H_{4g}$ and the principal term in its wave function is given by the Slater determinant

$$|\bar{\delta}_{+2u}\bar{\phi}_{+3u}| \tag{2}$$

and by the corresponding Slater determinant with all angular momenta reversed. These second degenerate wave functions will be omitted from here on since only one of them is necessary to derive our conclusions. A bar over the orbital denotes a β spin, the $|\lambda|$ value is given by the Greek letter, and the λ value is given by the numerical subscript. The subscript g or u is added to denote even or odd parity, respectively. Similarly the principal term in the $^3\Pi_{2g}$ wave function is given by the Slater determinant

$$|\bar{\delta}_{+2u}\bar{\phi}_{-3u}| \tag{3}$$

The only difference between the determinants of the two states is the spatial part of the second electron, $\phi_{+3} \rightarrow \phi_{-3}$. Both of these orbitals are ungerade in linear symmetry, so the transition is forbidden. If, however, some gerade character mixes into one or both of these orbitals the transition may become allowed.

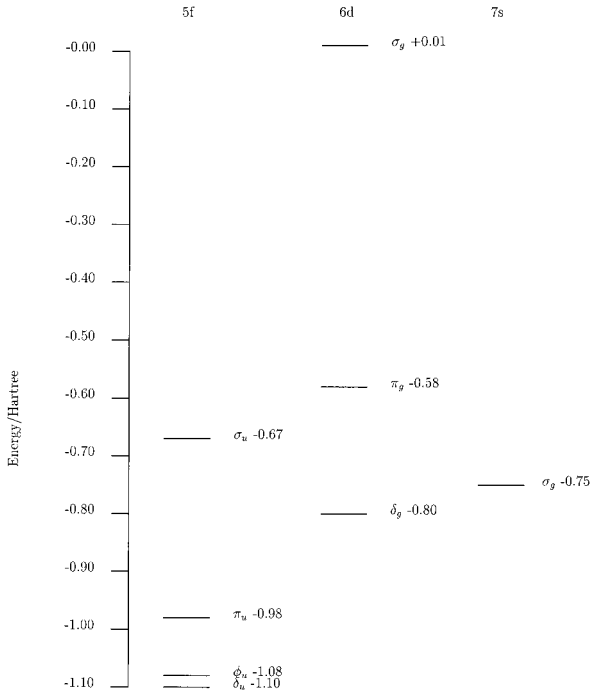

Figure 4. Typical orbital energy levels from an improved virtual orbital calculation for neptunyl.

An n-fold crystal field can be expanded in a Fourier series as

$$V_n(\mathbf{r}) = \sum_{i=0}^{\infty} A_{ni}(r,\vartheta)\cos(ni\varphi) \tag{4}$$

where φ is measured from the position of one of the vertical reflection planes so that there are no $\sin(ni\varphi)$ terms. Rules have been given[44] for expanding the combined ϑ, φ dependence in spherical harmonics if there is a need to do so. If n is even each term in $V_n(\mathbf{r})$ has gerade symmetry and inversion still commutes with the Hamiltonian. If n is odd, the terms have alternating parity $(-1)^{ni}$, and the ungerade terms prevent inversion from commuting with the Hamiltonian. The $A_0(r,\vartheta)$ term is expected to be the largest and tends to raise the energy of orbitals with large $|\lambda|$ since they have their largest amplitudes in or near the equatorial plane. The $i = 1$ term for odd values of n is the largest term with ungerade symmetry and can thus provide the ungerade-gerade mixing of orbitals and states necessary to make transitions electric-dipole allowed.

The orbitals available in the ground state for mixing are the $f\delta_u$ and $f\phi_u$. The virtual orbitals with gerade symmetry which are closest in energy are the Np 6d orbitals with the $d\delta_g$ the lowest.[45] The $d\delta_g$ orbitals are nonbonding, because they cannot mix with oxygen orbitals due to symmetry, but the $d\pi_g$ and $d\sigma_g$ are antibonding, in the same way the $f\pi_u$ and $f\sigma_u$ are, and thus higher in energy. A typical orbital energy pattern is shown in Figure 4. Mixing $5f\delta_u$ with $6d\delta_g$ requires an ungerade crystal field term with $n = 0$ or 4, which do not exist. Mixing $5f\phi_u$ with $6d\delta_g$ requires an ungerade crystal field term with $n = 1$ or 5.

If a 1-fold crystal field causes the mixing, the nonzero matrix elements are $\langle f\phi_{\pm 3u}|V_1|d\delta_{\pm 2g}\rangle$. Then the $d\delta_{\pm 2g}$ orbitals have to give nonzero electric-dipole transition moment matrix elements with some of the f orbitals. Within the (δ_u,ϕ_u) space, this can lead only to a nonzero electric-dipole transition moment of the ground state with itself. Because the ground state can mix with the $^1\Gamma_{4g}$ state, having the same Ω value, the transition to the

$^1\Gamma_{4g}$ gains some intensity. Indeed, in our calculations of NpO_2^+ with one chloride, the most intense transition is to the $^1\Gamma_{4g}$ state, but the intensity is not very high.

If a 5-fold crystal field is present the matrix elements $\langle f\phi_{\pm 3u}|V_5|d\delta_{\mp 2g}\rangle$ cause the mixing. The states that mix with the ground state because of the $\langle f\phi_{+3u}|V_5|d\delta_{-2g}\rangle$ ($=\langle f\phi_{-3u}|V_5|d\delta_{+2g}\rangle$) matrix element are

$$^3\Sigma_{1u}^{\pm}: \frac{1}{\sqrt{2}}(|\bar{\delta}_{+2u}\bar{\delta}_{-2g}| \pm |\bar{\delta}_{-2u}\bar{\delta}_{+2g}|) \tag{5}$$

(and the corresponding reversed wave functions). The ground-state becomes

$$|^3H'_{4g}\rangle = |^3H_{4g}\rangle - \frac{\langle ^3\Sigma_{1u}^+|V_5|^3H_{4g}\rangle}{E(^3\Sigma_{1u}^+) - E(^3H_{4g})}|\Sigma_{1u}^{3+}\rangle - \frac{\langle ^3\Sigma_{1u}^-|V_5|^3H_{4g}\rangle}{E(^3\Sigma_{1u}^-) - E(^3H_{4g})}|\Sigma_{1u}^{3-}\rangle \tag{6}$$

where $E(^3\Sigma_{1u}^{\pm})$ is the energy for the $^3\Sigma_{1u}^{\pm}$ states and $E(^3H_{4g})$ is the energy of the ground state. This energy difference has been calculated for the NpO_2^+ ion with a small spin−orbit CI calculation with 8 correlated electrons and has been found to be 39 008 cm^{-1} for the $^3\Sigma_{1u}^+$ and 44 721 cm^{-1} for the $^3\Sigma_{1u}^-$ state.

Furthermore, the excited $^3\Pi_{2g}$ state mixes through the crystal field with the $^3\Gamma_{3u}$ state:

$$|\bar{\delta}_{+2u}\bar{\delta}_{+2g}| \tag{7}$$

which is calculated to be 34 457 cm^{-1} above the ground state. The $^3\Pi_{2g}$ becomes

$$|^3\Pi'_{2g}\rangle = |^3\Pi_{2g}\rangle - \frac{\langle ^3\Gamma_{3u}|V_5|^3\Pi_{2g}\rangle}{E(^3\Gamma_{3u}) - E(^3\Pi_{2g})}|^3\Gamma_{3u}\rangle \tag{8}$$

We define the following abbreviations for the crystal field matrix element and the electric-dipole transition moment matrix elements

$$(V_5)_{\phi\delta} = \langle\phi_{\pm 3u}|V_5|\delta_{\mp 2g}\rangle \tag{9}$$

$$(\mu_\perp)_{\delta\phi} = \langle\delta_{\pm 2g}|\mu_\perp|\phi_{\mp 3u}\rangle \tag{10}$$

$$(\mu_{||})_{\delta\delta} = \langle\delta_{\pm 2g}|\mu_{||}|\delta_{\pm 2u}\rangle \tag{11}$$

For pure f and d functions, $(\mu_\perp)_{\delta\phi}/(\mu_{||})_{\delta\delta} = \sqrt{3/2}$. Using eqs 6 and 8−11, the transition moment becomes

$$\langle ^3H'_{4g}|\mu_\perp|^3\Pi'_{2g}\rangle = -\frac{1}{2}(V_5)_{\phi\delta}(\mu_\perp)_{\delta\phi}\left[\frac{1}{E(^3\Sigma_{1u}^+) - E(^3H_{4g})} + \frac{1}{E(^3\Sigma_{1u}^-) - E(^3H_{4g})} + \frac{2}{E(^3\Gamma_{3u}) - E(^3\Pi_{2g})}\right] \tag{12}$$

The last term will be even more effective than the first two because the denominator is only about 25 000 cm^{-1}.

The mixing of the ground state with the $^3\Sigma_{1u}^{\pm}$ states can give intensities not only to the $^3\Pi_{2g}$ but also to $^3\Pi_{0^+g}$, $^3\Pi_{0^-g}$, and $^3\Sigma_{1g}^-$. The wave functions for these states are

$$^3\Pi_{0\pm g}: \frac{1}{\sqrt{2}}(|\delta_{+2u}\phi_{-3u}| \pm |\bar{\delta}_{-2u}\bar{\phi}_{+3u}|) \tag{13}$$

$$^3\Sigma_{1g}^-: |\bar{\delta}_{+2u}\bar{\delta}_{-2u}| \tag{14}$$

The electric-dipole transition moments for the first two are

$$\langle ^3H'_{4g}|\mu_\perp|^3\Pi_{0\pm g}\rangle = \pm\frac{1}{2\sqrt{2}}(V_5)_{\phi\delta}(\mu_\perp)_{\delta\phi}\left[\frac{1}{E(^3\Sigma_{1u}^+) - E(^3H_{4g})} - \frac{1}{E(^3\Sigma_{1u}^-) - E(^3H_{4g})}\right] \tag{15}$$

These transitions are much weaker than the $^3\Pi_{2g}$ transition because there are only two terms instead of three and, even more importantly, these two terms have opposite signs. Because the $^3\Sigma_{1u}^+$ is close to $^3\Sigma_{1u}^-$ in energy, these terms almost cancel each other.

The transition to the $^3\Sigma_{1g}^-$ state is parallel:

$$\langle ^3H'_{4g}|\mu_{||}|^3\Sigma_{1g}^-\rangle = -\frac{1}{2}\frac{(V_5)_{\phi\delta}(\mu_{||})_{\delta\delta}}{E(^3\Sigma_{1u}^-) - E(^3H_{4g})} \tag{16}$$

Again this transition is not as intense as the one to $^3\Pi_{2g}$ because there is no mixing in the excited state. The $^3\Sigma_{1g}^-$ state though, mixes with other gerade states with $\Omega = 1$, giving them borrowed intensity. The $^3\Sigma_{1g}^-$ state is close to 3000 cm^{-1} and is not observed experimentally, because experimental absorption spectra have not been taken at such low energies. In our calculations though, it has considerable intensity. $^3\Pi_{1g}$ is close to 8000 cm^{-1}, mixes with $^3\Sigma_{1g}^-$, and is observed experimentally. We calculate a 42% mixing with the $^3\Sigma_{1g}^-$ and a high intensity. Even $^1\Pi_{1g}$ has some mixing with $^3\Sigma_{1g}^-$ and its calculated intensity is high. This state is close to 16 000 cm^{-1} where again experimental peaks are observed.

Transitions to states with $\Omega = 2$, $^3\Phi_{2g}$ and $^3\Delta_{2g}$, can become allowed by mixing with the $^3\Pi_{2g}$ through spin−orbit coupling. The mixing of the $^3\Delta_{2g}$ state is larger and thus it has larger intensity. Since the oscillator strength for the $^3\Pi_{2g}$ state is so large, even a small amount of mixing can give significant intensity to other states.

4.7. $NpO_2^{2+} + 5\ H_2O$. In an effort to test whether the above analysis of transition intensities applies to the other actinyl ions, we performed some calculations on $NpO_2(H_2O)_5^{2+}$. The geometry was provided by Blaudeau[36] who optimized it as described previously.

The R_e(Np−(axial O)) and R_e(Np−(equatorial O)) distances are 1.75 and 2.46 Å respectively. The five water molecules are aligned parallel to the NpO_2^{2+} axis as in NpO_2^+ and the symmetry is D_{5h}. The bond distances are similar to experimental[46] and other theoretical[29] results.

We will restrict our analysis to the $f \rightarrow f$ transitions. In particular the first four states, which are δ_u and/or ϕ_u in character can be useful in comparing with solution spectra. If the ground state is mostly $^2\Phi_{5/2u}$, as in the free ion case,[8] our analysis predicts two transitions. The ground-state wave function is $|\bar{\phi}_{+3u}|$. If mixing due to the field is taken into account, the $^2\Phi_{5/2u}$ becomes

$$|^2\Phi'_{5/2u}\rangle = |^2\Phi_{5/2u}\rangle - \frac{\langle ^2\Delta_{5/2g}|V_5|^2\Phi_{5/2u}\rangle}{E(^2\Delta_{5/2g}) - E(^2\Phi_{5/2u})}|^2\Delta_{5/2g}\rangle \tag{17}$$

and $^2\Phi_{7/2u}$ becomes

$$|^2\Phi'_{7/2u}\rangle = |^2\Phi_{7/2u}\rangle - \frac{\langle ^2\Delta_{3/2g}|V_5|^2\Phi_{7/2u}\rangle}{E(^2\Delta_{3/2g}) - E(^2\Phi_{7/2u})}|^2\Delta_{3/2g}\rangle \tag{18}$$

The allowed transitions will be

$$\langle {}^2\Phi'_{5/2u}|\mu_\perp|{}^2\Phi'_{7/2}\rangle = -(\mu_\perp)_{\delta\phi}(V_5)_{\phi\delta}\left[\frac{1}{E({}^2\Delta_{3/2g}) - E({}^2\Phi_{7/2u})} + \frac{1}{E({}^2\Delta_{5/2g}) - E({}^2\Phi_{5/2u})}\right] \quad (19)$$

$$\langle {}^2\Phi'_{5/2u}|\mu_{||}|{}^2\Delta_{5/2u}\rangle = -\frac{(V_5)_{\phi\delta}(\mu_{||})_{\delta\delta}}{E({}^2\Delta_{5/2g}) - E({}^2\Phi_{5/2u})} \quad (20)$$

The same type of orbitals as in NpO_2^+ mix with the ground-state orbitals. The states $^2\Delta_{3/2g}$ and $^2\Delta_{5/2g}$ are calculated respectively to be 52 332 cm^{-1} and 57 226 cm^{-1} higher than the ground state. The first transition will be more intense since there are two terms contributing. Each of these terms is probably larger than the term in the second transition, since $(\mu_\perp)_{\delta\phi}$ is greater than $(\mu_{||})_{\delta\delta}$ and perpendicular transitions have an intensity weighting factor of 2 compared to parallel transitions.

If the δ_u orbital is low enough compared to the ϕ_u orbital, then the ground state in linear symmetry would be a $^2\Delta_{3/2u}$ state, and one parallel transition to $^2\Phi_{7/2u}$ would be predicted.

$$\langle {}^2\Delta_{3/2u}|\mu_{||}|{}^2\Phi'_{7/2u}\rangle = -\frac{(\mu_{||})_{\delta\delta}(V_5)_{\phi\delta}}{E({}^2\Delta_{3/2g}) - E({}^2\Phi_{7/2u})} \quad (21)$$

The absorption spectrum of NpO_2^{2+} in aqueous solution has two peaks,[6] one at 6760 cm^{-1} with extinction coefficient ϵ_{max} = 5 M^{-1} cm^{-1}, and one at 8180 cm^{-1} with ϵ_{max} = 45 M^{-1} cm^{-1}. This spectrum fits with our analysis if $^2\Phi_{5/2u}$ is the ground state. The excited states, $^2\Delta_{5/2u}$ and $^2\Phi_{7/2u}$, are found experimentally[47] and theoretically[8] at approximately 6000−7000 cm^{-1} and 6500−9500 cm^{-1} respectively.

When we tried to calculate these states though, we found the $^2\Delta_{3/2u}$ as the ground state. When five equatorial ligands are around NpO_2^{2+}, the ϕ_u orbital is destabilized more than the δ_u orbital.[48] In our calculations this destabilization brings the $^2\Delta_{3/2u}$ lower. It should be mentioned that the character of the ground state is quite sensitive to correlation.[48] Since we do not include much correlation in these calculations of the hydrated neptunyl ion, we should be cautious about our results.

Transition energies and oscillator strengths are given in Table 8. In D_{5h} double group symmetry, $5/2_u$ wave functions transform as $E_{5/2}$, $3/2_u$ wave functions as $E_{7/2}$ and $7/2_u$ wave functions as $E_{3/2}$. The transition moments from the first excited state in our calculations, which is the ground state in the free ion, were calculated also, and are given in Table 9.

These calculations agree with our previous analysis. From the $^2\Phi_{5/2u}$ there is one parallel transition to $^2\Delta_{5/2u}$ and one perpendicular transition to $^2\Phi_{7/2u}$, whereas from the $^2\Delta_{3/2u}$ state there is only one intense parallel transition to $^2\Phi_{7/2u}$. The calculations predict a small transition from $^2\Delta_{3/2u}$ to $^2\Delta_{5/2u}$ as well.

From these results it is not conclusive what the ground state of the neptunyl ion in aqueous solution is. On one hand, in theory, the two lowest states are very close in energy which makes calculating the ground state difficult. On the other hand, spectra at energies as low as 7000 cm^{-1}, where the first absorption on NpO_2^{2+} is observed, are difficult to measure accurately because of the very high absorption of water. Small differences in cell/reference temperature or balancing may yield small false peaks. Only Waggener[49] has reported a spectrum at such low energies. He did the experiments in heavy water solutions in order to try to avoid the above problems. Still, given the potential difficulties, we have some reservations about assigning the ground state of neptunyl based entirely on this spectrum.

TABLE 8: Transition Energies and Intensities for NpO_2^{2+} + 5 H_2O from the Ground State, $E_{7/2}$

D_{5h}	$D_{\infty h}$	T_e (cm^{-1})	f (10^{-7})	mechanism
$E_{7/2}$	$^2\Delta_{3/2u}$	0	-	
$E_{5/2}$	$^2\Phi_{5/2u} + {}^2\Delta_{5/2u}$	717	0	
$E_{5/2}$	$^2\Delta_{5/2u} + {}^2\Phi_{5/2u}$	5415	0.4	$\mu_\perp$
$E_{3/2}$	$^2\Phi_{7/2u}$	7666	111.7	$\mu_{||}$

TABLE 9: Transition Energies and Intensities for NpO_2^{2+} + 5 H_2O from the $E_{5/2}$ State

D_{5h}	$D_{\infty h}$	T_e (cm^{-1})	f (10^{-7})	mechanism
$E_{5/2}$	$^2\Phi_{5/2u} + {}^2\Delta_{5/2u}$	0	-	
$E_{7/2}$	$^2\Delta_{3/2u}$	−717	0	
$E_{5/2}$	$^2\Delta_{5/2u} + {}^2\Phi_{5/2u}$	4698	61.8	$\mu_{||}$
$E_{3/2}$	$^2\Phi_{7/2u}$	6949	176.1	$\mu_\perp$

Conclusions

The oscillator strengths for transitions of NpO_2^+ with different numbers of equatorial ligands have been calculated. The experimentally observed spectrum can only be reproduced with five equatorial ligands. Crystal-field theory analysis shows that the initially forbidden transitions become allowed by mixing of the $5f\phi$ orbitals with $6d\delta$ orbitals. The same mechanism is operative for the other actinyl ions.

Acknowledgment. We thank David Clark and John Berg for suggesting aspects of this work and for helpful discussions of the literature. We thank Isaiah Shavitt, Hans Lischka, and Zhiyong Zhang for helpful discussions on the implementation of intensities within the GUGA formalism. S. M. was supported by a Presidential Fellowship from The Ohio State University. This work was supported in part by Pacific Northwest National Laboratory (PNNL) through Contract 200210, U.S. Department of Energy, the Mathematical, Information, and Computational Science Division, High-Performance Computing and Communications Program of the Office of Computational and Technology Research and by Argonne National Laboratory through the Actinide Synchrotron Studies project and through the Nuclear Energy Research Initiative (NERI) program, DOE Office of Nuclear Energy, Science, and Technology. PNNL is operated by Battelle Memorial Institute under contract DE-AC06-76RLO 1830. We used computational facilities at The Ohio State University (largely provided by the PNNL grant).

References and Notes

(1) Fahey, J. A., Neptunium. In *The Chemistry of the Actinide Elements*, 2nd ed.; Katz, J. J., Seaborg, G. T., Morss, L. R., Eds.; Chapman and Hall: London, 1986; Chapter 6, pp 443−498.

(2) Burney, G. A.; Harbour, R. M. *Radiochemistry of Neptunium;* U.S. Atomic Energy Commission, 1974.

(3) Hagan, P. G.; Cleveland, J. M. *J. Inorg. Nucl. Chem.* **1966**, *28*, 2905−2909.

(4) Sjoblom, R.; Hindman, J. C. *J. Am. Chem. Soc.* **1951**, *73*, 1744−1751.

(5) Friedman, H. A.; Toth, L. M. *J. Inorg. Nucl. Chem.* **1980**, *42*, 1347−1349.

(6) Carnall, W. T. Absorption and luminescence spectra. In *Gmelin Handbooks of Inorganic Chemistry, Transuranium Elements A2*, 8th ed.; Verlag Chemie GMBH: Weinheim/Bergstrasse, 1973; Chapter 8.2, pp 49−80.

(7) Keller, C. *The Chemistry of the Transuranium Elements;* Vol. 3; Verlag Chemie GMBH: Weinheim/Bergstrasse, 1971.

(8) Matsika, S.; Pitzer, R. M. *J. Phys. Chem. A* **2000**, *104*, 4064−4068.

(9) Denning, R. G.; Morrison, I. D. *Chem. Phys. Lett.* **1991**, *180*, 101−104.
(10) Zhang, Z.; Pitzer, R. M. *J. Phys. Chem. A* **1999**, *103*, 6880−6886.
(11) Ofelt, G. S. *J. Chem. Phys.* **1962**, *37*, 511−520.
(12) Judd, B. R. *Phys. Rev.* **1962**, *127*, 750−761.
(13) Ryan, J. L. Absorption spectra of actinide compounds. In *Lanthanides and Actinides*, Vol. 7 of *Inorganic chemistry Series one*; Bagnall, K. W., Eds.; Butterworths: London, 1972; pp 323−367.
(14) Sevost'yanova, E. P.; Khalturin, G. V. *Radiokhimiya* **1976**, *6*, 870−876.
(15) Tananaev, I. G. *Radiokhimiya* **1990**, *32*, 53−57.
(16) Neck, V.; Runde, W.; Kim, J. I.; Kanellakopulos, B. *Radiochim. Acta* **1994**, *65*, 29−37.
(17) Bessonov, A. A.; Afonas'eva, T. V.; Krot, N. N. *Radiokhimiya* **1990**, *32*, 24−31.
(18) Bessonov, A. A.; Afonas'eva, T. V.; Krot, N. N. *Radiokhimiya* **1990**, *32*, 32−35.
(19) Bessonov, A. A.; Krot, N. N. *Radiokhimiya* **1991**, *33*, 35−46.
(20) Bessonov, A. A.; Afonas'eva, T. V.; Krot, N. N. *Radiokhimiya* **1991**, *33*, 47−52.
(21) Grigor'ev, M. S.; Baturin, N. A.; Bessonov, A. A.; Krot, N. N. *Radiochemistry* **1995**, *37*, 12−14.
(22) Bessonov, A. A.; Krot, N. N.; Budantseva, N. A.; Afonas'eva, T. V. *Radiochemistry* **1996**, *38*, 210−212.
(23) Garnov, A. Y.; Krot, N. N.; Bessonov, A. A.; and Perminov, V. P. *Radiochemistry* **1996**, *38*, 402−406.
(24) Allen, P. G.; Bucher, J. J.; Shuh, D. K.; Edelstein, N. M.; Reich, T. *Inorg. Chem.* **1997**, *36*, 4676−4683.
(25) Conradson, S. D. *Appl. Spectrosc.* **1998**, *52*, 252A−279A.
(26) Eisenstein, J. C.; Pryce, M. H. L. *J. Res. Natn. Bur. Stand. A* **1966**, *70*, 165−173.
(27) Eisenstein, J. C.; Pryce, M. H. L. *J. Res. Natn. Bur. Stand. A* **1965**, *69*, 217−235.
(28) Herzberg, G. *Molecular Spectra and Molecular Structure. Spectra of Diatomic Molecules*, 2nd Ed.; Krieger Publishing Company: Malabar, Florida; Vol. 1, 1950.
(29) Hay, P. J.; Martin, R. L.; Schreckenbach, G. *J. Phys. Chem. A* **2000**, *104*, 6259−6270.
(30) Christiansen, P. A.; Ermler, W. C.; Pitzer, K. S. *Annu. Rev. Phys. Chem.* **1985**, *36*, 407−432.
(31) See http://www.clarkson.edu/~pac/reps.html for references and library of potentials.
(32) Yabushita, S.; Zhang, Z.; Pitzer, R. M. *J. Phys. Chem. A*, **1999**, *103*, 5791−5800.
(33) Shepard, R.; Shavitt, I.; Pitzer, R. M.; Comeau, D. C.; Pepper, M.; Lischka, H.; Szalay, P. G.; Ahlrichs, R.; Brown, F. B.; Zhao, J. *Int. J. Quantum Chem.: Quantum Chemistry Symposium* **1988**, *22*, 149−165.
(34) For information on the COLUMBUS programs see www.itc.univie.ac.at/~hans/Columbus/columbus.html.
(35) Blaudeau, J. P.; Brozell, S. R.; Matsika, S.; Zhang, Z.; Pitzer, R. M. *Int. J. Quantum Chem.* **2000**, *77*, 516−520.
(36) Blaudeau J. (private communication).
(37) Amsterdam Density Functional (ADF) code, Version 2.3.0, Department Theor. Chem., Vrije Universiteit, Amsterdam.
(38) Baerends, E. J.; Ellis, D. E.; Ros, P. *Chem. Phys.* **1973**, *2*, 41−51.
(39) te Velde, G.; Baerends, E. J. *J. Comput. Phys.* **1992**, *99*, 84−98.
(40) Cauchetier, P.; Guichard, C.; and Hucleux, M. Dosage du neptunium − applications aux solutions du retraitement chimique; In *Analytical Methods in the Nuclear Fuel Cycle*, pages 433−445. International Atomic Energy Agency publication, 1972; Symposium proceedings, Vienna, 1971.
(41) Sullivan, J. C. *J. Am. Chem. Soc.* **1965**, *87*, 1495−1498.
(42) Robinson, G. W. Electronic spectra. In *Methods of Experimental Physics*; Williams, D., Ed.; Academic Press: New York, 1962; pp 155−267.
(43) Basile, L. J.; Sullivan, J. C.; Ferraro, J. R.; LaBonville, P. *Appl. Spec.* **1974**, *28*, 142−145.
(44) Watanabe, H. *Operator Methods in Ligand Field Theory;* Prentice-Hall: Englewood Cliffs, New Jersey, 1966.
(45) Eisenstein, J. C.; Pryce, M. H. L. *Proc. R. Soc. London* **1955**, *A229*, 20−38.
(46) Clark, D. L.; Keogh, D. W.; Conradson, S. D.; Morales, L. A.; Neu, M. P.; Palmer, P. D.; Rogers, R. D.; Runde, W.; Scott, B. L.; Tait, C. D. Structural trends in actinyl(V, VI) ions of U, Np, and Pu; In *Book of Abstracts, 217th ACS National Meeting, Anaheim, Calif.*, NUCL-042, 1999.
(47) Denning, R. G.; Norris, J. O. W.; Brown, D. *Mol. Phys.* **1982**, *46*, 287−323.
(48) Matsika, S.; Pitzer, R. M. *J. Phys. Chem. A*, in press.
(49) Waggener, W. C. *J. Phys. Chem.* **1958**, *62*, 382−383.